POTENTIAL ENERGY MODEL FOR TURBULENT ENTRAINMENT ACROSS DENSITY INTERFACE IN A LINEARLY STRATIFIED FLUID

E XUE-QUAN (鄂学全) AND WANG WEI (王 薇)

(*Institute of Mechanics, Academia Sinica, Beijing* 100080, *PRC*)

Received June 24, 1991.

ABSTRACT

A potential energy model is developed for turbulent entrainment in the absence of mean shear in a linearly stratified fluid. The relation between the entrainment distance D and the time t and the relation between dimensionless entrainment rate E and the local Richardson number are obtained. An experiment is made for examination. The experimental results are in good agreement with the model, in which the dimensionless entrainment distance D is given by $\bar{D} = A_i(\bar{S})^{-1/4}(\bar{f})^{1/2}(\bar{t})^{1/8}$, where A_i is the proportional coefficient, S is the dimensionless stroke, $\bar{f}$ is the dimensionless frequency of the grid oscillation, $\bar{t}$ the dimensionless time.

Keywords: turbulent entrainment, linearly stratified fluid.

I. INTRODUCTION

Phenomena of fluid stratification and turbulent entrainment across density interface widely exist in the ocean and atmosphere. The turbulent mixing or entrainment in a stably stratified fluid is of great interest to geophysical fluid-dynamicists because it is closely related to the control of water-quality, prediction of atmospheric environment and meteorology.

Since the first laboratory simulating experiments conducted by Rouse & Dodu[1] in 1955, using a planar oscillating grid as the turbulent energy source, a lot of investigations were done and a good few results were obtained. But theoretical analysis appears inadequate, and the agreement between the existing theoretical models[4–6] and the experimental results is not good. In general, these theoretical studies are of two kinds. The first proceeds from analysis of the turbulent kinetic energy equation and integrates the equation. Surface fluxes of energy are balanced by dissipation and motion against gravity during entrainment. This balance is parameterized by semiempirical constraints on the relationships between the turbulent kinetic energy production and dissipation. Some models can be constructed for the fraction of the turbulent kinetic energy available for entrainment. Linden (1975) assumed that the rate of change in the potential energy is proportional to that in the potential energy input by the grid and obtained the dependence of the entrainment distance D on time t:

$$D \propto \begin{cases} t^{\frac{2}{13}} & S \ll D \ll z_0, \\ t^{\frac{2}{15}} & D \gg z_0, \end{cases} \tag{1}$$

where S is the stroke of the grid oscillation, z_0 is the distance between the grid and the fluid surface. Long (1978) has offered several arguments pertaining to the problem of entrainment in order to close the set of equations consisting of the energy equation and the integrated buoyancy equation across the mixed layer and interfacial layer, and found

$$D = B_9 K^{\frac{1}{2}} N^{-\frac{7}{18}} t^{\frac{1}{9}}, \tag{2}$$

$$E = \frac{u_e}{K/D} = \alpha Ri_1^{-\frac{7}{4}}, \tag{3}$$

where $K = uz$, u is the rms turbulent velocity, $u_e = dD/dt$ is the entrainment velocity, N is the buoyancy frequency, B_9 and α are constants, Ri_1 is the local Richardson number. Using dimensional analysis, Barenblatt (1982) obtained

$$D \propto t. \tag{4}$$

The second theoretical approach to the entrainment process consists of numerical simulation, but so far few results are known. These theories cannot well describe the results obtained from the experiments under the corresponding conditions.

In this paper, we attempt to find a theoretical model to describe the behavior of turbulent entrainment without mean shear in a linearly stratified fluid. An experimental examination is made and a comparison between the two is given.

II. Theoretical Analysis

If a planar turbulent energy source (such as oscillating grid) produces turbulent mixing in a stably linearly stratified fluid, a mixed layer is formed and develops, whose thickness D increases with time (see Fig. 1). The turbulent energy equation for a mixed layer without mean shear can be written as

$$\frac{1}{2}\frac{\partial}{\partial t}\langle q^2\rangle + \frac{\partial}{\partial z}\left\langle \left(p'/\rho_0 + \frac{1}{2}q^2\right) w \right\rangle = -\frac{g}{\rho_0}\langle w\rho'\rangle - \varepsilon_t, \tag{5}$$

where $q^2 = u^2 + v^2 + w^2$; u, v and w are the horizontal and vertical turbulent velocities, respectively; ρ_0 is the mean density of fluid, p' the fluctuating pressure, ρ' the fluctuating density, ε_t the viscous dissipation.

Considering a long time process, i.e. steady case, integrating (5) across the mixed layer from the grid to the interface, we obtain

$$\left\langle \left(p'/\rho_0 + \frac{1}{2}q^2\right) w \right\rangle_{\rm int} = \left\langle \left(p'/\rho_0 + \frac{1}{2}q^2\right) w \right\rangle_{\rm grid} - \frac{g}{\rho_0}\int \langle w\rho'\rangle dz - \int \varepsilon_t dz. \tag{6}$$

Eq. (6) implies that the turbulent energy at the interface is the value input at the grid minus removed by the buoyancy flux and dissipation in the layer. It is the energy available at the interface that deepens the mixed layer. The mixing

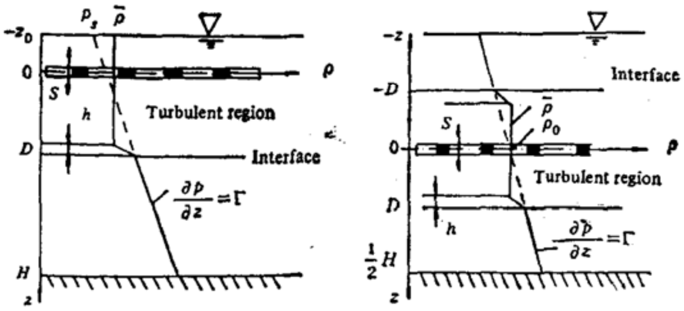

Fig. 1. Schematic diagram of the flow field described by the theory and the experimental arrangements.

causes redistribution of the fluid density, and changes the potential energy in the system. So we can assume that the rate of change of potential energy V (per unit horizontal area) of the fluid column is proportional to the vertical energy flux $d\varepsilon/dt$ per unit area available at the interface, i.e.

$$dV/dt = C_1 d\varepsilon/dt, \tag{7}$$

where C_1 is a proportional coefficient determined by experiments.

We shall establish this relationship. Now, we consider the entrainment behavior for grid positioned near the top and in the center of the linear density fluid column.

(1) *Grid near the top*

Consider a stratified fluid where the density ρ is given by

$$\rho = \begin{cases} \bar{\rho} & (-z_0 < z < D), \\ \rho_S + \Gamma(z + z_0) & (D \leqslant z \leqslant H), \end{cases} \tag{8}$$

when the grid is positioned near the top, where Γ is the density gradient constant. In general, the thickness of the interface layer h is very small compared with the entrainment distance (depth or thickness of the mixed layer) and can be neglected, so we have

$$\bar{\rho} = \frac{\Gamma}{2}(D + z_0) + \rho_S. \tag{9}$$

The potential energy of the fluid column is determined by

$$V = \int_{-z_0}^{H} g\rho z dz = \frac{1}{12} g\Gamma(D + z_0)^3 + \text{constant}. \tag{10}$$

Differentiating (10) with respect to time, we have

$$\frac{dV}{dt} = \frac{1}{4}\bar{\rho}N^2(D + z_0)^2 \frac{dD}{dt}, \tag{11}$$

where $N^2 = \Gamma \frac{g}{\bar{\rho}}$ is the buoyancy frequency.

The vertical energy flux $d\varepsilon/dt$ available at the interface, which is inputted by the grid, is $\frac{1}{2}\bar{\rho}w_I^3$, where w_I is the rms. vertical velocity of the turbulent motions, which is related to the rms. horizontal velocity at the density interface, according to Carruthers & Hunt[7]:

$$w_I^2 = au_I^2\left(\frac{u_I}{ND}\right)^{\frac{2}{3}}, \tag{12}$$

where a is a proportional coefficient, approximately 0.873. The rms. horizontal velocity of turbulence generated by the grid is given by[6]

$$u = CS^{\frac{3}{2}}M^{\frac{1}{2}}fz^{-1}, \tag{13}$$

where C is a constant, approximately 0.30, S (cm) is the stroke of the grid oscillation, f the frequency of the grid oscillation, z the distance measured from the center plane of the grid, and M (cm) the size of mesh.

When $z = D$, $u = u_I$, substituting (13) into (12), we have

$$\frac{d\varepsilon}{dt} = \frac{1}{2}a^{3/2}C^4\bar{\rho}S^6M^2f^4N^{-1}D^{-5}. \tag{14}$$

Substituting (11) and (14) into (7), we find

$$(D + z_0)^2D\frac{dD}{dt} = 2C_1a^{3/2}u_I^4N^{-3}, \tag{15}$$

or

$$(D + z_0)^2D^5\frac{dD}{dt} = 2C_1C^4a^{3/2}S^6M^2f^4N^{-3}. \tag{16}$$

For smaller time process after starting the grid. i.e. $D \ll z_0$ and for long time process i.e. $D \gg z_0$, integrating (16), we obtain respectively

$$D = A_1SM^{1/3}f^{2/3}N^{-1/2}t^{1/6}, \quad D \ll z_0, \tag{17}$$

$$D = A_1S^{3/4}M^{1/4}f^{1/2}N^{-3/8}t^{1/8}, \quad D \gg z_0, \tag{18}$$

where A_1 is a proportional coefficient determined by experiment. These are the dependence of the entrainment on the time. At the long timescale, the entrainment distance increases with 1/8 power of time. These formulas again indicate the dependence of the entrainment distance on the stratified property (N) and the external parameters generating turbulent source.

Let us consider turbulent entrainment rate. Differentiating (18) with respect to time, we obtain the entrainment rate

$$u_e = \frac{dD}{dt} = \frac{1}{8}A_1S^{3/4}M^{1/4}f^{1/2}N^{-3/8}t^{-7/8}. \tag{19}$$

It is shown that the entrainment rate u_e decreases with 7/8 power of time. The local Richardson number is defined as

$$Ri_1 = N^2\bigg/\left(\frac{u_I}{l}\right)^2, \tag{20}$$

where $l = \beta D$ is the integral length scale, β is the constant, approximately 0.10 at $S/M \leqslant 0.8$. (Hopfinger & Toly, 1976). When $D \gg z_0$, using (13) and (19), we get the dimensionless entrainment rate $E(=u_e/u_l)$:

$$E = K_1 Ri_l^{-3/2}, \tag{21}$$

where K_1 is a constant determined by experiment. The dimensionless entrainment rate decreases with 3/2 power of the Richardson number Ri_l.

Eqs. (18), (19) and (21) describe zero-mean-shear turbulent entrainment law in situations of turbulent energy source near the top.

(2) *Grid in the center*

When the grid is placed in the center (Fig. 1(b)), $z_0 = 0$ and $\bar{\rho} = \rho_0$.

As above, the potential energy per unit area of fluid column is given by

$$V = \frac{1}{3} g\Gamma D^3 + \frac{2}{3} \Gamma H^3 \rho_0 g. \tag{22}$$

The rate of change in the potential energy is

$$\frac{dV}{dt} = g\Gamma D^2 \frac{dD}{dt} = \rho_0 N^2 D^2 \frac{dD}{dt}. \tag{23}$$

Considering $u = u_l$ at $z = D$, the vertical energy flux available at the interface is given by $\frac{1}{2}\rho_0 w_l^3$. From (12), (13), (23) and (7) we obtain the relation between the entrainment distance and the time:

$$D = A_2 S^{3/4} M^{1/4} f^{1/2} N^{-3/8} t^{1/8}, \tag{24}$$

and the entrainment rate:

$$u_e = \frac{1}{8} A_2 S^{3/4} M^{1/4} f^{1/2} N^{-3/8} t^{-7/8}, \tag{25}$$

where A_2 is a constant determined by experiment. Eqs. (24) and (25) are of the same form with (18) and (19), respectively.

Using the same method we get the relation between the dimensionless turbulent rate E and the Richardson number Ri_l:

$$E = K_2 Ri_l^{-3/2}, \tag{26}$$

where K_2 is the proportional coefficient determined by experiment. This formula is the same as (21).

The relationships above show that in the linearly stratified fluid, the entrainment behavior for the turbulent energy source near the top and for that in the center can be described by the same relationship.

III. Experimental Examination

In order to examine the theoretical model, an experiment was carried out in a transparent plexiglass tank of 52 cm × 52 cm in cross-section and 72 cm in height, equipped with a grid of 2 cm square bars, aligned in a square array of mesh $M=10$ cm. The grid placed horizontally in the tank could be oscillated vertically. The stroke and frequency of grid oscillation could be adjusted. The oscillating mechanism was described in Ref. [8].

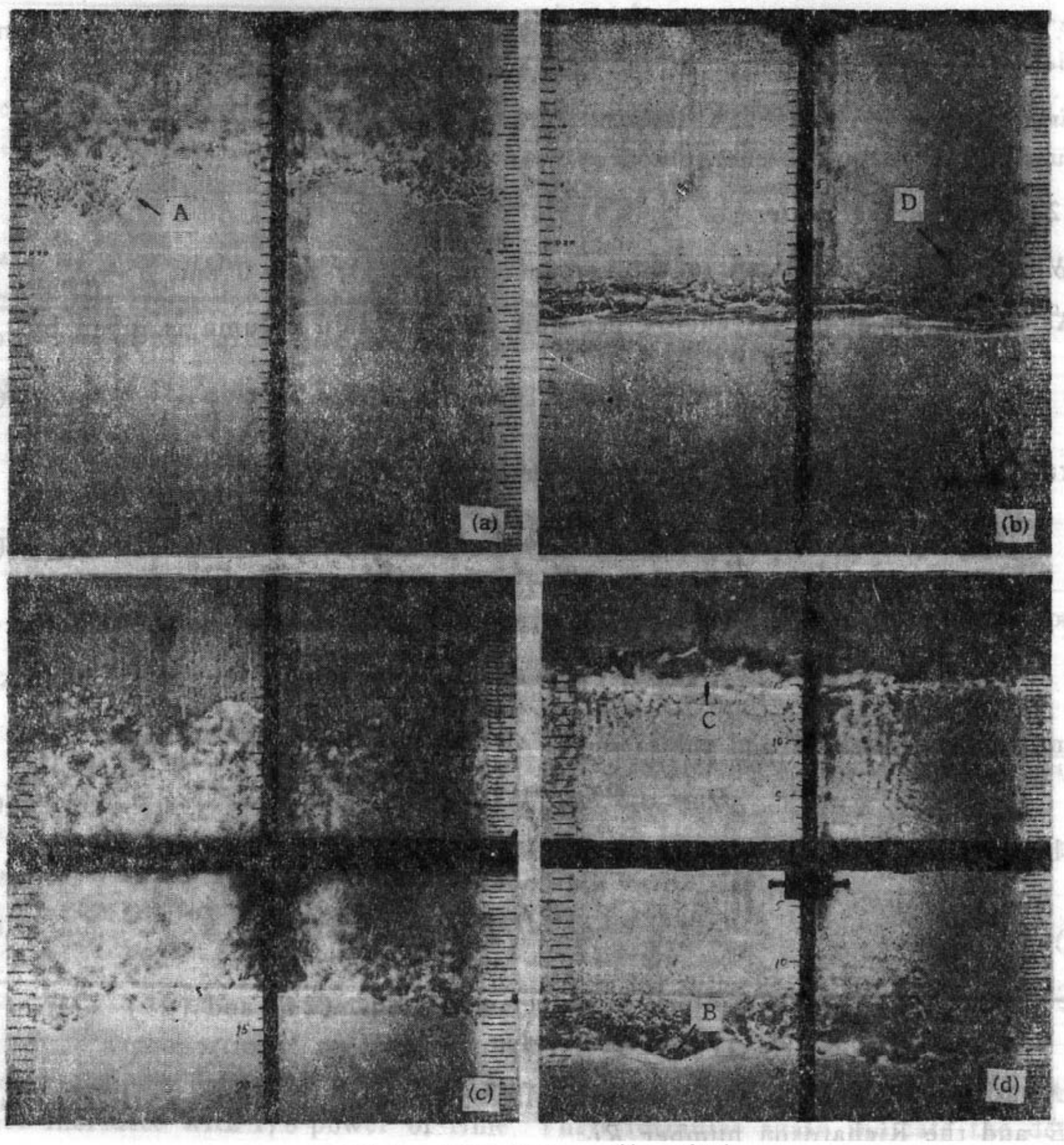

Fig. 2. Flow patterns ($f=6$ Hz).
Grid at the top: $N=0.6766$, (a) $t=9$ s, (b) $t=1328$ s. Grid in the center: $N=0.6945$, (a) $t=4$ s, (b) $t=88$ s.
A, The turbulent front; B, the internal wave; C, the interfacial layer; D, the flow filaments.

Salt water of various densities was allowed to flow into the bottom of the tank via a special set-up, and the required buoyancy frequencies were obtained. The experimental method was simple. Experiments were begun by simultaneously starting the grid oscillation and the electronic timer. The position of the turbulent front and the time were recorded on a shadowgraph for determining the entrainment rate (see Ref.[8]). The reading error was smaller than 2 mm, the time error was not larger than 0.1s.

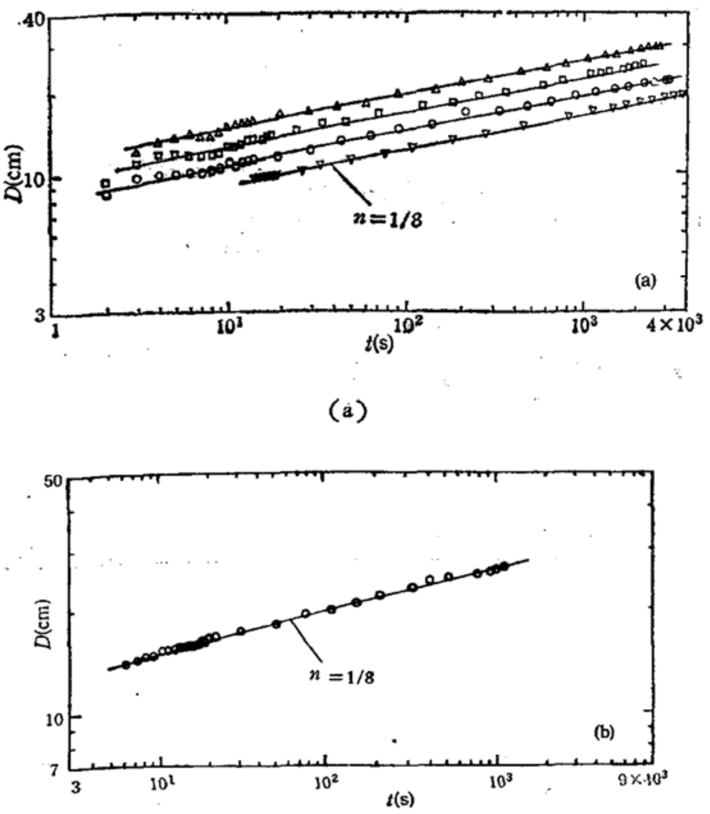

(a)

(b)

Fig. 3. Variation of the turbulent entrainment distance with time ($S = 2$ cm)
(a) Grid at the top: ▽, $f = 2.3$ Hz; ○, $f = 3.3$ Hz; □, $f = 4.3$ Hz; △, $f = 6$ Hz.
(b) Grid in the center: ○, $f = 6$ Hz; —, the present model.

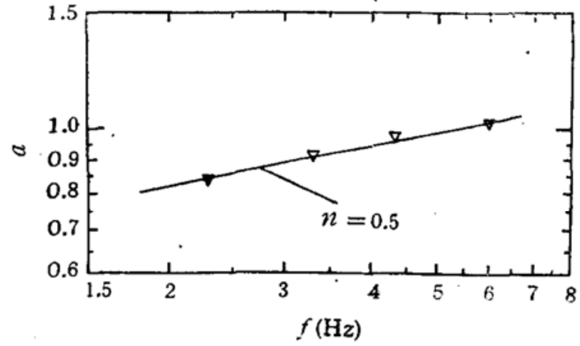

Fig. 4. Relation between the coefficient a and frequency f. —, The present model.

The experimental parameters were $S=2$ cm, $M=10$ cm, $f=3$—6 Hz, $z_0=6$c m, $H = 55$ cm. $N = 0.667\ \mathrm{s}^{-1}$. The results are given in Fig.2—Fig.6.

IV. Results and Discussion

(1) *Flow visualization*. Fig. 2 is the flow pattern of the turbulent motions. When the grid started oscillating, the turbulent motions were violent, and a turbulent layer formed and grew rapidly, the turbulent front distorting and moving up and down violently (Fig. 2(a),(c)). This implies that the turbulent eddies are energetic and entrain fluid. After the turbulent front reached a certain distance,

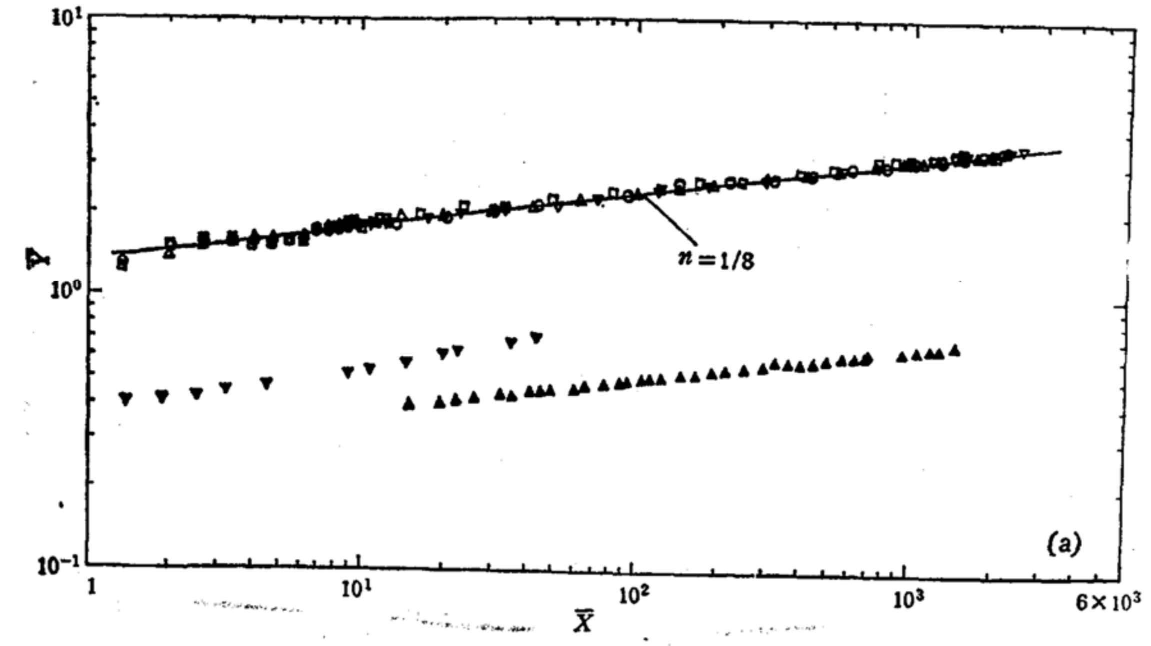

(a)

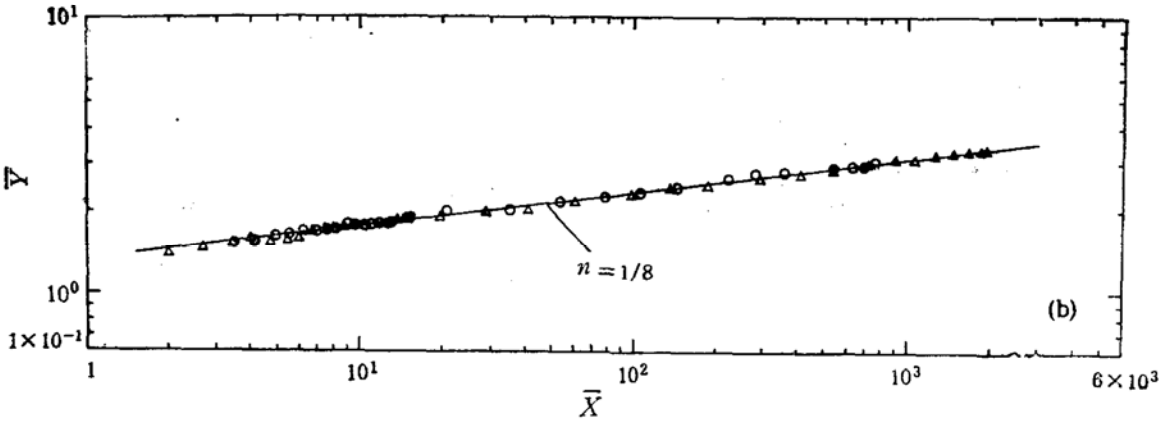

(b)

Fig. 5. Non-dimensionalized mixed-layer thickness Y versus non-dimensionalized time.

$$\left(\overline{Y}=\frac{D}{S\left(\frac{M}{S}\right)^{1/4}\left(\frac{f}{N}\right)^{1/2}},\ \overline{X}=Nt\right)$$

(a) Grid at the top: ▽, $f=2.3$ Hz; ○, $f=3.3$ Hz; □, $f=4.3$ Hz; △, $f=6$ Hz. ▼, Lin der (1975); ▲, Folse and Schexnayder (1981). (b) $f=6$ Hz: △, grid at the top; ○, grid in the center. —, the present model.

the motions of the turbulent front became gentle and stable, and the density-interfacial layer was clearly visible (Fig.2(b),(d)). Intheinterfacial layer, internal waves appear to form and break down ceaselessly, obvious fluid filaments being seen rising from the interface; it causes mixing and makes the mixed layer grow gradually.

(2) *Dependence of the entrainment on time*. The entrainment distance increases with the time. It is seen from (18) and (24) that the entrainment distance D increases by 1/8 power of time. This entrainment law is suitable for the case where the planar turbulent energy source is near the top or in the center of line-

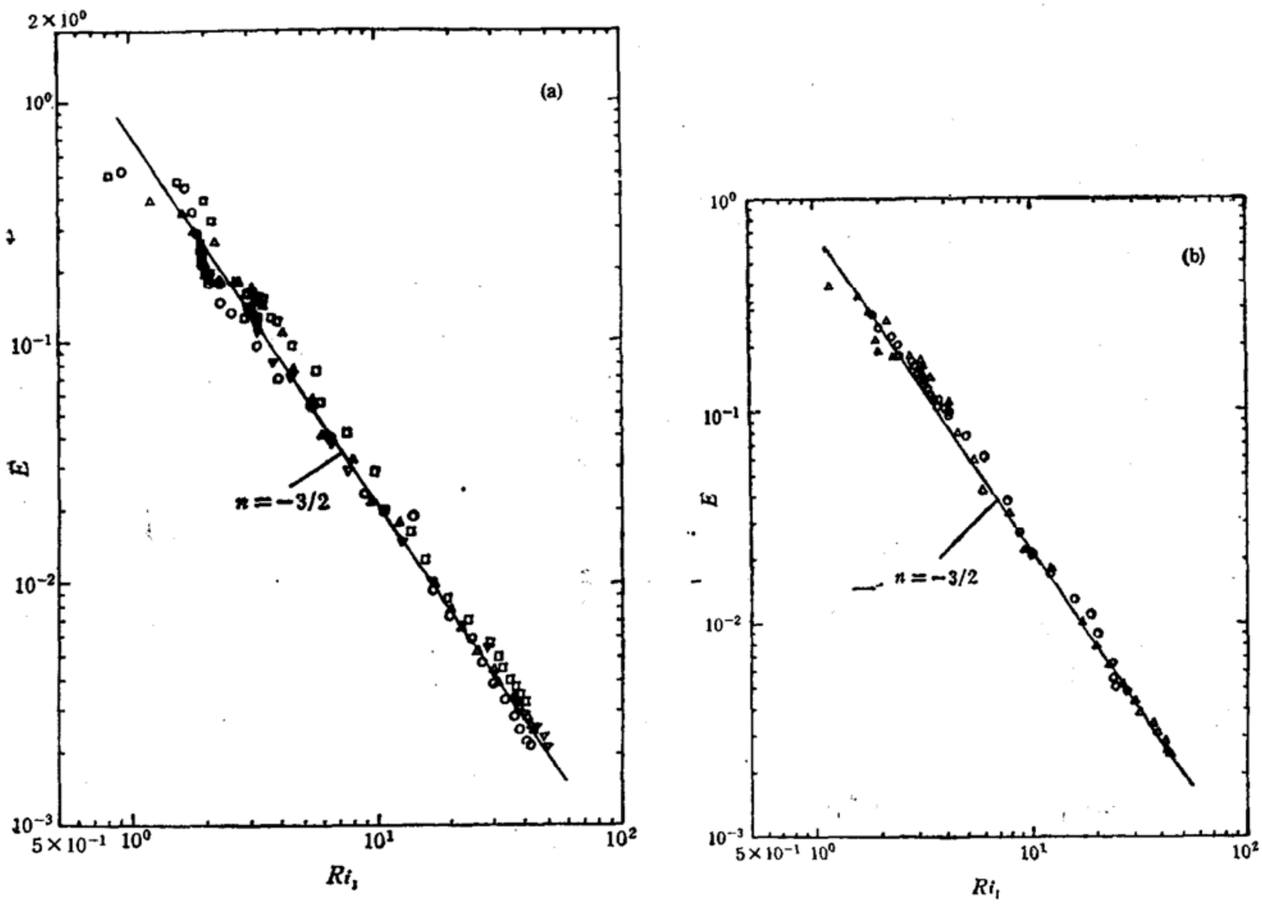

Fig. 6. Variation of E with Ri_1.
(a) Grid at the top. (b) grid in the center. (For caption, see Fig. 5.)

arly stratified fluid. Fig.3 well shows that the experimental data are in excellent agreement with the theory. This is consistent with the experimental results obtained by E Xue-guan and Hopfinger[3]. The constants determined by experiments A_1 and A_2 are 1.3099 and 1.3240 (1.5599 in Ref. [3]), respectively. Our D-t relation ($D \propto t^{1/8}$) is different from Linder's $D \propto t^{2/15}$ (second equation of (1)) and Long's $D \propto t^{1/9}$. The power of time in our D-t relation is between theirs, while the difference of their power of time is great (0.022), which makes their curves diverged and the deviation of D increases with time.

(3) *Relation between the entrainment distance and the stratification property.* The stratification is characterized by the buoyancy frequency N. The entrainment distance D changes by $-3/8$ power of N, i.e. $D \propto N^{-3/8}$, as given in (18) and (24). Comparing the relation $D \propto N^{-3/8}$ with Long's $D \propto N^{-7/18}$ and Linden's $D \propto N^{-4/15}$, we can see that the power of N is close to the former, but quite different from the latter. Careful analysis of the measured results obtained by Folse (1981)[9] shows that the exponent of N is close to $-3/8$.

(4) *Relations between the entrainment distance and the grid parameters.* (18) and (24) obviously indicate the dependence of D on S, M and f. The theory (potential energy model) is supported by the results in Ref. [3] and verified by

this experiment (Fig.4).

(5) *Dimensionless entrainment rate.* We can find a relationship between the dimensionless entrainment rate and the dimensionless parameters by dimensional analysis. Eqs. (18) and (24) can be written as

$$\frac{D}{S} = A_i\left(\frac{M}{S}\right)^{1/4}\left(\frac{f}{N}\right)^{1/2}(Nt)^{1/8}, \tag{27}$$

or

$$\bar{D}(\bar{S})^{1/4}(\bar{f})^{-1/2} = A_i(\bar{t})^{1/8}, \tag{28}$$

where $\bar{D} = D/S$, $\bar{S} = S/M$ and $\bar{f}=Nf$ are the dimensionless entrainment distance, stroke and frequency of the grid oscillation, respectively, A_i ($i = 1$ for the grid near the top, $i = 2$ for the grid in the center) is the constant related to the size of the grid bar, $A_i = 1.31$ for this experiment. All the measured data can fall on a curve (Fig.5). Some other experimental results cited in Fig.5 show that (27) is correct. Those curves are low, because the size of used bar of the grid is smaller, thus A_i takes smaller value.

(6) *The turbulent entrainment rate.* Eqs. (19) and (25) show the dependence of the entrainment rate on the time, stratification property and grid parameters. The theory gives the relation between the dimensionless entrainment rate E and local Richardson number Ri_1, $E \propto Ri_1^{-3/2}$ (see (21) and (26)), which agrees with the experimental results (Fig.6) and those of Ref.[3] and Breidenthal[10]. K_1 and K_2 in (21) and (26) are 0.7101 and 0.7489, respectively.

We do not discuss the case of $D \ll z_0$ because this process is very rapid and we are interested in the long time process.

V. Conclusions

The principal results of the theory are presented below.

(1) The potential energy model based on the energy balance, suggested by the paper can well describe the features of the turbulent entrainment without mean shear in a linearly stratified fluid.

(2) For the case where the planar turbulent source is positioned near the top or in the center of the linearly stratified fluid, the theoretical model has the same expression. This shows that for the linearly stratified fluid, the entrainment characteristics are the same and independent of the position of the turbulent source. This is quite different from the two-layer fluid system.

(3) This model includes the relations between the various parameters. The entrainment distance D varies with $S^{3/4}$, $M^{1/4}$, $f^{1/2}$, $N^{-3/8}$ and $t^{1/8}$, which is expressed in dimensionless form as $\bar{D} = A_i(\bar{S})^{-1/4}(\bar{f})^{1/2}(\bar{t})^{1/8}$. The dimensionless turbulent ertrainment varies with $-3/2$ power of local Richardson number: $E = K_i Ri_1^{-3/2}$.

(4) In linearly stratified fluid, when the turbulent mixed zone begins to form, its initial growth is very rapid due to the effect of convection near the grid. In

this zone, the relations between the entrainment distance and time are different, such as $D \propto t^{1/2}$[11], t^{1}[6], $t^{2/13}$[3,4] and $t^{1/6}$ for the model. So it is necessary to further study the initial growth process of the mixed zone.

References

[1] Rouse, H. & Dodu, J., *Turbulent Diffusion Across a Density Discontinuity*, Houille Blanche, **10**(1955), 522—532.

[2] Hopfinger, E. J. & Toly, J. A., Spatially decaying turbulence and its relation to mixing across density interface, *J. Fluid Mech.*, **78**(1976), part 1, 155.

[3] E Xuequan & Hopfinger, E. J., On mixing across an interface in stably stratified fluid, *J. Fluid Mech*, **166**(1986), 227.

[4] Linden, P. F., The deepening of a mixed layer in a stratified fluid, *J. Fluid Mech*, **71**(1975), part 2,385.

[5] Long R. R., A theory of mixing in a stably stratified fluid, *J. Fluid Mech.*, **84**(1978), part 1, 113.

[6] Barenblatt, G. I., *Similarity, Self-Similarity and Intermediate Asymptotics—Theory and Application to Geophysical Hydrodynamics* (in Russian), Leningrad Gidrometeoizdat 1982, 209—223.

[7] Carruthers, D. J. & Hunt, J. C. R. Velocity fluctuation near an interface between a turbulent region and a stably stratified layer, *J. Fluid Mech.*, **165**(1986), 475.

[8] E Xuequan & Wang Wei, The growth of a mixing layer with suspended solid particles in a two-layer fluid system. Submitted to *Science in China*, 1991.

[9] Folse, R. F., Cox, R. P. & Schexnayder, K. R., Measurements of the growth of a turbulently mixed layer in a linearly stratified fluid, *Phys. Fluids.*, **24**(1981), 396.

[10] Breidenthal, R. E. & Baker, M. B. Convection and entrainment across stratified interfaces, *J. Geoph. Res.* **90**(1985), **13**(D7) 055—13,062.

[11] Fernando, H. J. S. The growth of a turbulent part in a stratified fluid, *J. Fluid Mech.*, **190** (1988), 55.